

THIS IS A PREPRINT --- SUBJECT TO CORRECTION

## An Evaluation of Acid Fluid Loss Additives, Retarded Acids, and Acidized Fracture Conductivity

By

D. E. Nierode, Member AIME, and K. F. Kruk, Esso Production Research Co.

© Copyright 1973

American Institute of Mining, Metallurgical, and Petroleum Engineers, Inc.

This paper was prepared for the 48th Annual Fall Meeting of the Society of Petroleum Engineers of AIME, to be held in Las Vegas, Nev., Sept. 30-Oct. 3, 1973. Permission to copy is restricted to an abstract of not more than 300 words. Illustrations may not be copied. The abstract should contain conspicuous acknowledgment of where and by whom the paper is presented. Publication elsewhere after publication in the JOURNAL OF PETROLEUM TECHNOLOGY or the SOCIETY OF PETROLEUM ENGINEERS JOURNAL is usually granted upon request to the Editor of the appropriate journal provided agreement to give proper credit is made.

Discussion of this paper is invited. Three copies of any discussion should be sent to the Society of Petroleum Engineers office. Such discussion may be presented at the above meeting and, with the paper, may be considered for publication in one of the two SPE magazines.

### ABSTRACT

An evaluation of acid additives and retarded acid systems indicates that the stimulation resulting from acid fracturing can be increased when effective fluid loss additives are used in HCl, or when the acid viscosity is increased significantly. Acid emulsions were found to have a low fluid loss rate and to be retarded, whereas oil wetting surfactants gave no retardation at typical field injection rates. Conductivity studies show that, in general, the fracture flow capacity resulting from acid reaction is very high, except when rock embedment strength and/or rock solubility is low, or the closure stress is high.

### INTRODUCTION

In an acid fracturing treatment, either acid alone is injected into the formation at a high rate, or the acid is preceded by a viscous fluid (the pad fluid) to form a long, wide fracture. When acid is used without a pad fluid, the fracture will generally be short and narrow since the rate of fluid loss for acid is high. If a viscous pad fluid is used, the long, wide fracture that is formed will begin to close as acid is injected, and will approach the geometry expected if acid alone had been used. This decrease in fracture volume occurs because the

References and illustrations at end of paper.

acid wormholes through the region invaded by the viscous fluid and thereby increases the rate of fluid loss.

The stimulation obtained in an acid fracturing treatment is controlled by the length of the fracture that is effectively acidized, not by the induced fracture length. The distance reactive acid moves along the fracture (the acid penetration distance) is governed by the acid flow rate along the fracture, the rate of acid transfer to the fracture wall, and the reaction rate at the rock surface. It has been shown<sup>1,2</sup> that under most circumstances, the reaction rate between acid and rock is very fast, and that the rate of mass transfer to the rock face controls the overall acid reaction rate.<sup>3</sup>

A design procedure that combines the previously discussed fracturing aspects with the reaction behavior of acid has been recently developed<sup>3</sup> and compared with field treatment results.<sup>4</sup> The design method considers the bounds on the acid penetration distance (the fluid loss limit and the reaction rate limit) shown in Fig. 1. The fluid loss limit is estimated assuming the benefits of the pad fluid are lost instantaneously through the formation of wormhole channels and is identical to the penetration calculated if no pad fluid is used. The reaction rate limit is the theoretical maximum acid penetration distance. It is calculated assuming the pad fluid

can control the rate of fluid loss after acid is injected and that the acid-rock reaction rate controls the extent of acid penetration. Unfortunately, field treatment data<sup>4</sup> correlate with the fluid loss limit, indicating that the rate of acid fluid loss from the fracture controls the stimulation attained from the acid fracturing process.

As a result of these prior studies, it has been concluded that the most urgent improvement needed in acid fracturing is better fluid loss control when acid is injected.

Even with controlled acid fluid loss, normal acid fracturing treatments are limited due to excessive reaction rate if the reservoir temperature is greater than about 250°F. Under these conditions, retardation is needed to reduce the reaction rate and increase the acid penetration distance. The need for acid retardation has long been appreciated;<sup>5,6</sup> however, a new dynamic test procedure<sup>3</sup> has cast doubt on the validity of past retarded acid testing methods.

To attain high stimulation ratios, it is necessary that the acidized fracture conductivity be high.<sup>7</sup> Fortunately, it has been found that when acidized, most carbonates yield highly conductive fractures;<sup>4,8</sup> however, many formations either do not respond to acid fracturing, or quickly lose stimulation due to suspected fracture closure. Prior researchers<sup>8</sup> have studied the conductivity generated in a smooth-walled system where the prime mechanism for creation of conductivity is uneven reaction due to rock heterogeneities. Measured conductivities have been on the order of  $10^4$ - $10^6$  md in, showing that the effect of rock heterogeneity is quite important. It is anticipated that even in homogeneous formations, the conductivity resulting from the smoothing of peaks and valleys on the rough fracture faces can generate a highly conductive fracture.

In this paper, we present studies designed to evaluate the following: (1) fluid loss characteristics of emulsified acids and hydrochloric acid containing acid fluid loss additives, (2) the reactivity of emulsified acids and acids containing oil wetting surfactants, and (3) the conductivity generated when homogeneous-rough walled cores are acidized.

#### ACID FLUID LOSS CHARACTERISTICS

The rate of acid fluid loss from a fracture was evaluated in a laboratory test where acid was forced through a carbonate core at a constant differential pressure. An oil saturated core with a residual brine saturation was flooded with acid, acid containing a fluid loss additive, or an emulsified acid as required in the test of interest. The fluid and core were preheated to 200°F. Indiana limestone cores 2 inches in

diameter and 12 inches long were used in all tests. Further experimental details are presented in Appendix I, and test results are summarized in Table 1.

Since in most acid fracturing treatments a viscous pad is injected prior to the acid, experiments were conducted initially to indicate the degree of fluid loss control provided by the pad fluid. In these experiments, tests 1 and 2 in Table 1, the rate of HCl fluid loss was compared for a core saturated with a 200 cp oil and a 1 cp oil. Each core contained a residual water saturation of about 25 percent. At a differential pressure of 500 psi, the time to wormhole breakthrough when the core was saturated with the 1 cp oil was 2250 sec; when saturated with a 200 cp oil, breakthrough occurred in 2340 sec. The respective pore volumes of acid injection at breakthrough were 1.2 and 0.5.

These data show that the viscous pad fluid reduced the average leakoff velocity by a factor of 2.5 in this test, not 200-fold as would be predicted assuming the pad fluid controlled flow velocity. It is even more important to note that the time required for the wormhole to penetrate through the core in the two experiments was essentially the same, so that the average wormhole growth rate through the 12-inch cores was about equal. These experiments lend support to the field verified concept that acid is quickly able to wormhole through the viscous pad fluid adjacent to the fracture, thereby causing the rate of acid fluid loss to be controlled by the spent acid viscosity.

Eight commercially available acid fluid loss additives listed in Table 2 were evaluated using the test procedure described in Appendix I. Of these additives, only Additive A, a mixture of two finely ground oil soluble resins,<sup>9</sup> significantly reduced the rate of acid fluid loss under lab test conditions. Tests 3 through 9 in Table 1 show that as the concentration of Additive A is increased, breakthrough time for the wormhole is at first reduced and then substantially increased, when compared to HCl without additive. The pore volumes of acid injected prior to breakthrough show a similar trend, while the average leakoff velocity is increased at low additive concentrations, but is significantly reduced at concentrations of about 200 lb/1000 gal.

The effectiveness of Additive A is dramatically reduced as the pressure gradient is increased, as shown by tests 7 and 9. These results show that at a concentration of 200 lb of Additive A/1000 gal of acid, all benefit would be lost if the pressure gradient were greater than 200 psi per inch. No other additives tested demonstrated even this degree of fluid loss control at 200°F. It is possible, however, that at temperatures below 200°F, other products would also have shown some fluid loss reduction and

that Additive A would be more efficient.

A more general way to reduce the rate of acid fluid loss appears to be through the use of viscous acids. Tests 10 through 12 in Table 1 show that a viscous, acid external emulsion,<sup>10</sup> designated AE1, has a low rate of fluid loss, apparently as a result of its high viscosity, and that the addition of a commercially available fluid loss additive at concentrations up to 200 lb/1000 gal further reduces leakoff rate.\*

It is currently not possible to rigorously scale these data to field conditions, since the number and spacing of wormholes leaving the fracture face cannot be predicted. In the tests described in this paper, we always found only one wormhole in each core (1 wormhole per 20.5 cm<sup>2</sup>). It is possible that the actual wormhole spacing under field conditions could be as low as 0.01 or 0.001 times this value with a correspondingly reduced leakoff velocity. Fluid loss tests using cores with a larger surface area are currently underway to determine the proper scaling procedure.

The fluid loss tests reported in this paper, though not directly usable to design field treatments, are at least qualitative indications that Additive A and the acid external emulsion fluid reduce the rate of fluid loss. To evaluate the effectiveness of these substances, several field tests were conducted for comparison to treatments where an acid fluid loss additive was not used. Fig. 2 shows that jobs using Additive A gave a stimulation more nearly in agreement with the reaction rate limit, whereas treatments without Additive A gave stimulation ratios in good agreement with the fluid loss limit. (Treatment specifics are summarized in Table 3.) In other words, the additive restricted acid leak-off and allowed live acid to penetrate farther along the fracture. It is important to note that the fracture propagation pressure in these wells was less than 2000 psi. As previously noted, the particulate additive is probably not effective in formations where the filtration pressure exceeds 2400 psi.

Field tests of AE1, a newly developed acid external emulsion, show that improved stimulation is obtained when the emulsion is used as a pad fluid ahead of plain HCl. A comparison of treatments without an acid fluid loss additive to two treatments where the acid emulsion was used is given in Fig. 3. Here again, as in Fig. 2 for Additive A, the acid penetration distance and stimulation ratio are increased to more nearly agree with the reaction rate limit. We attribute this increase to improved fluid loss control by the viscous acid. These particular

\* The fluid loss additive used in these tests is comprised of an inert particle coated with a guar-like coating.

tests were in dolomite formations with a bottom-hole temperature of about 120°F, so the results do not reflect the benefits of retardation, although the emulsified acid is retarded.

#### RETARDED ACIDS

Acids are retarded for acid fracturing purposes only if their reaction rate during flow along a fracture is significantly lower than the reaction rate of plain HCl. As previously indicated, it is also necessary that a retarded acid restrict the rate of acid fluid loss, for unless it does, the benefits of retardation will accrue in the rock matrix near the wellbore instead of along the fracture. Acids reported to be retarded were tested under laboratory conditions designed to accurately simulate reaction in the fracture. Tests were conducted during flow through a rough-walled fracture at elevated temperatures and pressures, and at field flow rates. (Test details are described in Appendix II.) Acids evaluated included viscous acids and acids containing oil wetting surfactants.

#### Viscous Acids

Of the acids tested, only viscous acids such as oil and acid external emulsions, and gelled acid, are retarded. The degree of retardation is indicated in Fig. 4 where the measured acid concentration is plotted as a function of distance along the rough-walled fracture. Acids included in the figure are plain 28 percent HCl, two oil-external emulsified acids, and an acid external emulsified acid. (The composition of these acids is given in Table 4.) This study is not intended to be an extensive study of retarded acid systems. Rather, we hope to indicate the general direction required to improve acidizing fluids and the test procedures required to accurately evaluate these fluids.

Since the high viscosity of emulsified acids provides the retardation,<sup>3</sup> it follows that emulsion stability must be maintained to have a retarded system. Data in Fig. 4 show that emulsion OE2 breaks after penetrating about 45 feet along the fracture, while the other emulsions are still stable after flowing 100 feet. Data in Fig. 4 also show that the oil external emulsions can have a dissolving power equivalent to about 18% HCl when 28% HCl is used as the acid phase, whereas similar acid external emulsions are limited to a dissolving power equivalent to 9% HCl. In some instances, this low dissolving power may limit fracture conductivity and thereby stimulation ratio.

As with hydrochloric acid, the reaction rate for emulsified acids can be correlated by assuming that acid reaction rate at the fracture wall is very fast, and finding the effective mixing coefficient required to fit the data (the detailed

procedure was first described by Williams and Nierode<sup>2</sup>). Effective mixing coefficients from tests with emulsified acids are compared to previously published data for HCl in Fig. 5. In this correlation, the Reynold's number,  $2Wu_0\rho/\mu$ , is evaluated for emulsion viscosity at the wall shear rate,  $6Q/H/W^2$ . Surprisingly, mixing coefficient data for the emulsified acids (both oil and acid external forms) are in reasonable agreement with the data for HCl obtained at comparable Reynold's numbers. One must recognize, however, that these Reynold's numbers correspond to injection rates lower than normally used with HCl alone. Small Reynold's numbers result with the viscous fluid since fluid viscosity appears in the denominator of the dimensionless group.

Although both types of emulsified acids exhibited retardation under laboratory conditions, the acid external system is more readily adapted to field operations. This acid can be pumped at relatively low friction pressure<sup>10</sup> whereas the oil external system inherently results in high friction pressure.

When HCl is gelled with commonly available polymers like guar, gum karaya, or a polyacrylamide, the resulting viscous acid is retarded so long as the fluid is viscous. Unfortunately, retardation in gelled acids is quickly lost as the gelling agent degrades with time and temperature. Fig. 6 shows that the viscosity of HCl gelled with 50 lb guar/1000 gal acid is less than 10 cp after 30 minutes at 100°F. A similar test run at 150°F is difficult to interpret quantitatively since the polymer degrades before the sample reaches test temperature. When bottom-hole temperature is less than 150°F, polymer addition to HCl in the range of 50-100 lb/1000 gal should provide some fluid loss control and retardation; however, the transient nature of the system makes its use undesirable from a field operational viewpoint.

#### Chemically Retarded Acids

The commercially available oil wetting surfactants tested in this study do not retard the reaction rate of HCl under acid fracturing field conditions, as shown in Fig. 7. The three additives tested reportedly function by forming a thin oil film over part of the fracture face, thus shielding some of the fracture area from reaction. When tested under static conditions, these additives do give significant retardation, however, indicating that the surfactant can form a stable oil film. Data in Fig. 7 show that in the limit of very low flow rates (below typical field rates), the reaction is retarded and small effective mixing coefficients are measured. This is in agreement with static data. At typical field flow rates, the reaction rate is equivalent to that for plain HCl and the effective mixing coefficients are equal within the range of experimental reproducibility. If

an effective surfactant is found, it is important to recognize that data discussed elsewhere in this paper and in prior publications would suggest that no benefit could result from its use unless it is used in combination with an effective fluid loss additive.

#### FRACTURE CONDUCTIVITY

##### Experimental Measurements

The conductivity of a fracture created by acid reaction is probably impossible to predict from first principles since it is a function of the rock strength, heterogeneities present in the rock, the volume and distribution of rock dissolved, and other variables. One estimate for the conductivity can be obtained by assuming the fracture walls are dissolved uniformly leaving an open channel of constant width. This conductivity, which we call the dissolved rock equivalent conductivity, DREC, is often higher than the observed value.

To evaluate the etched fracture conductivity under conditions believed to realistically represent field conditions, we developed a new test procedure (described in detail in Appendix III). In this test, a core plug is broken in tension to simulate the rough surface obtained in the field, is acidized as a vertical fracture, is subjected to a closure stress, and the conductivity is measured. Results of these tests are summarized in Table 5 and a representative plot of conductivity as a function of closure stress for a San Angelo Dolomite core plug is given as Fig. 8. It should be noted that most of the data in Table 5 are for DREC values less than  $10^7$  md-inches (expected field values can range as high as  $10^{10}$  md-in) since the core plugs usually broke if acidized further. The data thus must be extrapolated to the upper range of expected field values.

We believe the conductivity measured in these tests is mainly due to the smoothing of peaks and valleys on the rough fracture faces, and is independent of rock heterogeneities due to the small sample size. For many formations, several groups of samples were tested for different rock types encountered in the section. A few experiments that resulted in unusually high conductivities showed on later examination that the fracture face had been unevenly etched due to a heterogeneity. Since most reservoirs are heterogeneous, and since viscous fingering of acid through the pad fluid would further contribute to conductivity, we feel that our results represent a lower bound on the conductivity actually attained in the field.

The acidized fracture conductivity values tabulated in Table 5 can be correlated with the dissolved rock equivalent conductivity, DREC, and the rock strength as measured by the rock

embedment strength, RES.\* These correlations are shown in Figs. 9 and 10 where the experimental conductivity data are compared to curves representing the best least square fit of the data. Equations relating these correlations are given below.

$$wk_f = C_1 \exp \{-C_2 S\} \quad (1)$$

$$C_1 = 0.265 [\text{DREC}]^{0.822} \quad (2)$$

$$C_2 \times 10^3 = \begin{cases} 19.9 - 1.3 \ln (\text{RES}) & 0 < \text{RES} < 20,000 \text{ psi} \\ 3.8 - 0.28 \ln (\text{RES}) & 20,000 \leq \text{RES} \leq 500,000 \text{ psi} \end{cases} \quad (3)$$

where  $wk_f$  = fracture conductivity, md in

$S$  = fracture closure stress, psi

The expected change in conductivity with closure stress and rock strength is illustrated in Fig. 11 where Eqs. (1)-(3) are plotted for DREC =  $10^8$  md-in and closure stresses of 1000, 3000, and 5000 psi. These predictions show that if RES is very low, the points of support for the fracture will collapse and the resulting fracture will have a low conductivity, whereas if RES is high, conductivities in the  $10^5$ - $10^7$  range are obtained.

The conductivity correlation represented by Eqs. (1)-(3) can be used in conjunction with a model<sup>3</sup> for the acid fracturing process to predict the PI improvement expected from specific treatments. The producing closure stress,  $S$ , is easily calculated from formation characteristics and the producing bottom-hole pressure. DREC is calculated by an acid material balance after the acid concentration profile is predicted. The only parameter that is difficult to determine is RES since core material from the formation to be treated must be available. If core material is not available, one can select a measured value from Table 6 for a similar reservoir, or as a last resort, assume a value believed to characterize the rock.

The first two entries in Table 6 correspond to two of the reservoirs in which Nierode et al.<sup>4</sup> had previously compared observed stimulation results to experimental predictions. In that earlier work, it was assumed that the fracture had a conductivity of  $10^6$  md-inches or greater in every case. Calculations with Eqs. (1)-(3) for three successfully stimulated wells (Wells 9-11 in Table 7, Reference 4) show a large

\* Rock embedment strength has been defined as the force required to push a steel ball bearing into a rock surface to a distance equal to the radius of the ball, divided by the projected area of the bearing.

predicted fracture conductivity contrast (conductivity divided by bulk formation permeability) of  $7 \times 10^5$  inches, while similar calculations for a field where fracture collapse was strongly suspected (Wells 14-18, Table 7, Reference 4) show that expected contrast would be only about  $5 \times 10^2$  inches. Had the latter information been available earlier, these jobs would likely not have been done.

#### CONCLUSIONS

1. Effective fluid loss additives can significantly improve stimulation from an acid fracturing treatment. However, most commercially available particulate additives tested were ineffective at 200°F, and none were effective if the filtration pressure exceeded 2400 psi.
2. Viscous acids are retarded under acid fracturing field conditions, and in addition can provide excellent fluid loss control under some conditions. Emulsified acids, particularly the acid external emulsions, have wide application, whereas gelled acids currently are limited to bottom-hole temperatures less than about 150°F. The main limitation on the use of emulsified acids at high temperatures is their high tubular friction pressure, and in some instances their instability.
3. Chemically retarded acids are not retarded under field conditions.
4. The lower bound on fracture conductivity can be predicted from producing drawdown, rock embedment strength, and dissolved rock equivalent conductivity using correlations developed in this paper.

#### NOMENCLATURE

C	Acid concentration, moles/litre
$C_0$	Initial acid concentration, moles/litre
$C_1, C_2$	Constants in Eq. (1)
DREC	Dissolved rock equivalent conductivity, md-in
H	Fracture height, ft
$i^*$	Flow rate, $\text{cm}^3/\text{sec}$
L	Fracture length, ft
$\Delta m$	Change in mass, gm
$\Delta p$	Change in pressure, psi
Q	Flow rate, barrels/minute
RES	Rock embedment strength, psi
S	Closure stress, psi
$u_0$	Average flow velocity, ft/min
w	Fracture width, in
$wk_f$	Fracture conductivity, md-in
$\rho$	Density, $\text{lb}_m/\text{ft}^3$
$\mu$	Viscosity, cp

REFERENCES

1. Nierode, D. E., and Williams, B. B., "Characteristics of Acid Reaction in Limestone Formations," Soc. Pet. Eng. J., December, 1971, p. 406.
2. Roberts, L. D., and Guin, J. A., "The Effect of Surface Kinetics in Fracture Acidizing," SPE Preprint 4349.
3. Williams, B. B., and Nierode, D. E., "Design of Acid Fracturing Treatments," J. Pet. Tech., (July, 1972), 849.
4. Nierode, D. E., Bombardier, C. C. and Williams, B. B., "Prediction of Stimulation from Acid Fracturing Treatments," Can. J. Pet. Tech., (October-December, 1972).
5. Knox, J. A., Pollock, R. W., and Beecroft, W. H., "The Chemical Retardation of Acid and How It Can Be Utilized," Can. J. Pet. Tech., (January-March, 1965).
6. Smith, C. F., Crowe, C. W., and Wieland, D. R., "Fracture Acidizing in High Temperature Limestone," SPE 3008 presented at SPE 45th Annual Fall Meeting, Houston, October 4-7, 1970.
7. McGuire, W. J., and Sikora, V. J., "The Effect of Vertical Fractures on Well Productivity," Trans. AIME (1960) 219, 401-403.
8. Broaddus, G. C., and Knox, J. A., "Influence of Acid Type and Quantity in Limestone Etching," Mid-Continent API, Wichita, Kansas, March 31-April 2, 1965.
9. Crowe, C. W., "Evaluation of Oil Soluble Resin Mixtures as Diverting Agents for Matrix Acidizing," SPE Preprint 3505.
10. Sinclair, A. R., Terry, W. M., and Kiel, O. M., "Polymer Emulsion Fracturing," SPE 4675, to be presented at the 1973 Fall SPE Meeting.
11. McGlothlin, B. B., and Huitt, J. L., "Relation of Formation Rock Strength to Propping Agent Strength in Hydraulic Fracturing," SPE 1311 presented at SPE Petroleum Conference, Tulsa, Oklahoma, May 3-4, 1965.

APPENDIX I

ACID FLUID LOSS TEST PROCEDURE

Core Preparation

Indiana limestone cores 1-1/2 inches in diameter by 12 inches long were encased in heat shrinkable tubing and covered with a molded, 1/4 inch layer of epoxy resin. The resin layer was needed to prevent wormhole breakthrough at the cylindrical core surface, and subsequent sleeve failure of the Hassler core holder.

Test Procedure

The core was mounted in a conventional 2-inch Hassler core holder, evacuated, flooded with brine, flooded with diesel, and the permeability to diesel measured at room temperature. With pressure at 1000 psi, the system was heated for 4 hours at 200°F and the permeability to diesel again determined.

A test run consisted of establishing a constant pressure differential with diesel followed by a switchover to the acid system being investigated. Back pressure was in excess of 1000 psi, and pressure differential was held constant with a variable speed Ruska pump. Total time and displaced volume at breakthrough were measured as was the volumetric flow rate during the experiment.

APPENDIX II

RETARDED ACID TEST PROCEDURE

Test Cell

Reaction rate was measured during dynamic flow through a test cell containing a rough walled fracture 2 inches high and 5 ft long. Overall system pressure was maintained in excess of 1000 psi to keep CO<sub>2</sub> in solution, and flow rate was set in the range of expected field values. Test acid was flowed through the cell between Greer Accumulators, and valves were arranged so that acid could be recycled through the test cell to simulate flow along a fracture greater than 5 ft in length. Provisions were made to take pressurized input and output samples so that in situ viscosity could be measured, and so that the amount of evolved CO<sub>2</sub> could be determined as a measure of reaction rate.

Test Procedure

The test cell and acid accumulators were separately heated for at least 4 hours at test temperature. A test subrun consisted of flowing

all of the acid through the test cell at a prescribed rate and taking input and output samples to measure the amount of reaction during the run. The subrun was then repeated as many times as desired until a sufficient range of acid reaction was investigated. Since it took about 5 minutes to switch valves for the next subrun, samples were taken from the acid volume that resided in the fracture during the switchover, so that the final simulated acid concentration profile could be corrected for this extraneous reaction.

#### Data Analysis

If the acid tested was only slightly retarded, concentration change during a subrun was determined by ordinary acid-base or  $\text{Ca}^{++}$  titrations. When retardation was great, titration precision was so low that pressurized samples were instead analyzed for  $\text{CO}_2$  content by expansion into an evacuated, known volume. Amount of reaction occurring during the switching operation was similarly determined. The effective mixing coefficient was calculated from the measured concentration change during a subrun by Eq. (4).

$$D_e = \frac{3.46 w_i^* (1-C/C_o)^{3/2}}{LH} \times 10^{-5} \quad (4)$$

### APPENDIX III

#### CONDUCTIVITY TEST PROCEDURE

##### Core Preparation

Core plugs one inch in diameter and 2-3 inches long were fractured in tension in a press to simulate a rough walled fracture, and weighed. Core halves were then mounted in an acid frac-

turing test cell<sup>3</sup> and acidized under field conditions to simulate a vertical, acidized fracture. The core was then dried and again weighed so that the dissolved rock equivalent conductivity could be determined from Eq. (5).

$$\text{DREC} = 1.00 \times 10^6 \left[ \frac{\Delta m}{\rho LH} \right]_{\text{Rock}}^3 \quad (5)$$

##### Conductivity Measurement

The acidized core halves were encased in shim stock and a rubber sleeve, and mounted in a 10,000 psi Hassler core holder. Hydraulic sleeve pressure was applied to the core holder causing closure stress on the fracture given by Eq. (6).

$$S = \frac{2}{\pi} p_{\text{sleeve}} \quad (6)$$

At a particular sleeve pressure, 200 cp silicone oil was pumped through the fracture with a Ruska pump at three different flow rates, and the respective pressure drops were measured. Conductivity was calculated from Eq. (7) for each flow rate and the results were averaged.

$$wk_f = 5788 \frac{i * Lu}{\Delta p H} \quad (7)$$

The experiment was repeated at increasing sleeve pressures to a limiting pressure 10,000 psi, or until the conductivity was less than 10 md-inches.

An unfractured core plug and a fractured, but unacidized, plug were run in the apparatus to show that the shim stock-rubber sleeve combination effectively sealed. Both tests resulted in Darcy flow through the cores confirming a good peripheral seal.

TABLE 1 - FLUID LOSS TEST DATA\*\*

	Description of Experiment*	Pressure Differential psi	Time to Wormhole Breakthrough sec	Pore Volumes at Breakthrough	Average Fluid Velocity ft/min x 10 <sup>3</sup>	Average Wormhole Velocity ft/min x 10 <sup>2</sup>
1	1 cp oil in core--no fluid loss additive in acid	500	2,250	1.20	3.68	2.67
2	200 cp oil in core--no fluid loss additive in acid	500	2,340	0.50	1.47	2.56
3	no additive	500	2,850	0.82	1.99	2.10
4	15 lb A/1000 gallons	500	1,150	0.44	2.64	5.22
5	50 lb A/1000 gallons	500	2,320	0.80	2.38	2.59
6	100 lb A/1000 gallons	500	7,500	1.63	1.50	0.80
7	200 lb A/1000 gallons	500	28,800	3.00	0.72	0.21
8	no additive	1,700	180	0.50	19.20	33.33
9	200 lb A/1000 gallons	1,700	558	1.50	18.50	10.75
10	Emulsion <sup>t</sup> AE1, no additive	1,000	637	0.36	3.90	9.42
11	Emulsion <sup>t</sup> AE1, 100 lb silica flour/1000 gallons	1,000	980	0.64	4.51	6.12
12	Emulsion <sup>t</sup> AE1, 200 lb silica flour/1000 gallons	1,000	4,328	1.87	2.98	1.39
13	150 lb B/1000 gal	500	2,395	0.68	1.96	2.50
14	100 lb C/1000 gal	500	968	0.58	4.10	6.20
15	150 lb D/1000 gal	500	1,368	0.60	3.02	4.39
16	150 lb E/1000 gal	500	442	0.34	5.30	13.57
17	200 lb F/1000 gal	500	1,890	0.85	3.10	3.17
18	100 lb G/1000 gal	500	1,307	0.51	2.67	4.59
19	200 lb G/1000 gal	500	1,026	0.82	5.54	5.85
20	150 lb H/1000 gal	500	1,220	0.50	2.82	4.92

\* 15% HCl and diesel saturated core unless otherwise specified.

\*\* all tests were conducted at 200°F.

t see Table 4 for composition.

TABLE 2 - PARTICULATE FLUID LOSS ADDITIVES TESTED

Additive	Description
A	Mixture of two types of finely ground oil soluble resin.
B	Mixture of finely ground natural polymer and hydrocarbon resin.
C	Finely ground natural polymer.
D	Finely ground acid swellable polymer.
E	Finely ground silica flour-hydrocarbon mixture.
F	Benzoic acid flakes.
G	Rice hulls mixed with finely ground inert filler.
H	Oil soluble amorphous hydrocarbon mixed with acid swellable resin.



TABLE 3 - WELL DATA FOR ADDITIVE A TEST PROGRAM

Well	Depth ft	Gross/Net Thickness ft/ft	Permealility	Past Stimulation Treatments	Last Treatment	
					Pad Volume /Rate gal/BPM	Acid Volume /Rate gal/BPM
1	4,000	50/18	34	1000 gal 15% HCl	15,000/20	11,500/16
2	4,240	50/9	44	31,000# sand frac lost to gyp	15,000/10	10,000/15
3	4,000	50/17	30	500 gal 15% HCl	16,000/15	10,000/17
4	4,370	50/15	25	500 gal 15% HCl	10,000/7	10,000/12
5	4,250	50/13	18	500 gal 15% HCl	11,000/8	11,000 <sup>1</sup> /20
6	3,980	50/15	20	25,000# sand frac	11,000/12	11,000 <sup>2</sup> /12

<sup>1</sup>200 lb Additive A/1000 gal of acid

<sup>2</sup>150 lb Additive A/1000 gal of acid

TABLE 4 - VISCOUS ACID COMPOSITIONS

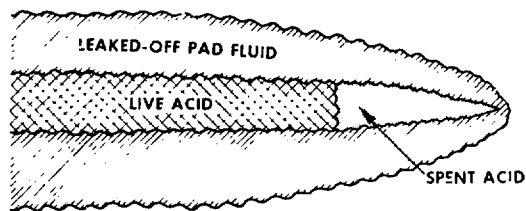
Acid Type	Description
AE1	Acid external emulsion consisting of 2 parts kerosene to 1 part 28% HCl, containing 2 lb guar per barrel of acid, and 1% proprietary emulsifier. <sup>11</sup>
OE1	Oil external emulsion consisting of 1 part kerosene to 2 parts 28% HCl with 4% (by oil volume) duodecylbenzene sulphonic acid emulsifier.
OE2	Oil external emulsion consisting of 1 part kerosene to 2 parts 28% HCl plus 0.5% (by oil volume) proprietary emulsifier.
Gelled HCl	15 percent HCl containing 50 lb guar/1000 gallons of acid.

TABLE 5 - CONDUCTIVITY DATA

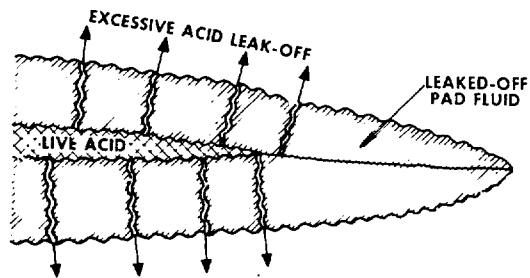
Formation	DREC md in	RES psi	Conductivity (md in) vs. Closure Stress (psi)				
			0	1,000	3,000	5,000	7,000
San Andres Dolomite	$2.7 \times 10^6$	76,600	$1.1 \times 10^4$	$5.3 \times 10^3$	$1.2 \times 10^3$	$2.7 \times 10^2$	$6.0 \times 10^0$
San Andres Dolomite	$5.1 \times 10^8$	63,800	$1.2 \times 10^6$	$7.5 \times 10^5$	$3.0 \times 10^5$	$1.2 \times 10^5$	$4.7 \times 10^4$
San Andres Dolomite	$1.9 \times 10^7$	62,700	$2.1 \times 10^5$	$9.4 \times 10^4$	$1.9 \times 10^4$	$3.7 \times 10^3$	$7.2 \times 10^2$
Canyon Limestone	$1.3 \times 10^8$	88,100	$1.3 \times 10^6$	$7.6 \times 10^5$	$3.1 \times 10^5$	$4.8 \times 10^4$	$6.8 \times 10^3$
Canyon Limestone	$4.6 \times 10^7$	30,700	$8.0 \times 10^5$	$3.9 \times 10^5$	$9.4 \times 10^4$	$2.3 \times 10^4$	$5.4 \times 10^3$
Canyon Limestone	$2.7 \times 10^8$	46,400	$1.6 \times 10^6$	$6.8 \times 10^5$	$1.3 \times 10^5$	$2.3 \times 10^4$	$4.4 \times 10^3$
Cisco Limestone	$1.2 \times 10^5$	67,100	$2.5 \times 10^3$	$1.3 \times 10^3$	$3.4 \times 10^2$	$8.8 \times 10^1$	$2.3 \times 10^1$
Cisco Limestone	$3.0 \times 10^5$	14,800	$7.0 \times 10^3$	$3.4 \times 10^3$	$8.0 \times 10^2$	$1.9 \times 10^2$	$4.4 \times 10^1$
Cisco Limestone	$2.0 \times 10^6$	25,300	$1.4 \times 10^5$	$6.2 \times 10^4$	$1.3 \times 10^4$	$2.7 \times 10^3$	$5.7 \times 10^2$
Capps Limestone	$3.2 \times 10^5$	13,000	$9.7 \times 10^3$	$4.2 \times 10^3$	$7.6 \times 10^2$	$1.4 \times 10^2$	$2.5 \times 10^1$
Capps Limestone	$2.9 \times 10^5$	30,100	$1.8 \times 10^4$	$6.8 \times 10^3$	$9.4 \times 10^2$	$1.3 \times 10^2$	$1.8 \times 10^1$
Indiana Limestone	$4.5 \times 10^6$	22,700	$4.6 \times 10^5$	$1.5 \times 10^5$	$1.5 \times 10^4$	$1.5 \times 10^3$	$1.5 \times 10^2$
Indiana Limestone	$2.8 \times 10^7$	21,500	$7.9 \times 10^5$	$3.0 \times 10^5$	$4.3 \times 10^4$	$6.5 \times 10^3$	$9.0 \times 10^2$
Indiana Limestone	$3.1 \times 10^8$	14,300	$7.4 \times 10^6$	$2.0 \times 10^6$	$1.4 \times 10^5$	$1.0 \times 10^4$	$7.0 \times 10^2$
Austin Chalk	$3.9 \times 10^6$	11,100	$5.6 \times 10^4$	$1.6 \times 10^3$	$1.3 \times 10^0$	-	-
Austin Chalk	$2.4 \times 10^6$	5,600	$3.9 \times 10^4$	$1.2 \times 10^3$	$1.2 \times 10^0$	-	-
Austin Chalk	$4.8 \times 10^5$	13,200	$1.0 \times 10^4$	$1.7 \times 10^3$	$4.9 \times 10^1$	$1.4 \times 10^0$	-
Clearfork Dolomite	$3.6 \times 10^4$	35,000	$3.4 \times 10^3$	$1.7 \times 10^3$	$4.1 \times 10^2$	$1.0 \times 10^2$	$2.4 \times 10^1$
Clearfork Dolomite	$3.3 \times 10^4$	11,800	$9.3 \times 10^3$	$1.6 \times 10^3$	$4.5 \times 10^1$	$1.3 \times 10^0$	-
Greyburg Dolomite	$8.3 \times 10^6$	14,400	$2.5 \times 10^5$	$4.0 \times 10^4$	$1.0 \times 10^3$	$2.5 \times 10^1$	-
Greyburg Dolomite	$3.9 \times 10^6$	12,200	$2.1 \times 10^5$	$7.9 \times 10^4$	$1.0 \times 10^4$	$1.5 \times 10^3$	$2.0 \times 10^2$
Greyburg Dolomite	$3.2 \times 10^6$	16,600	$8.0 \times 10^4$	$1.5 \times 10^4$	$4.8 \times 10^2$	$1.6 \times 10^1$	-
San Andres Dolomite	$1.0 \times 10^6$	46,500	$8.3 \times 10^4$	$4.0 \times 10^4$	$9.5 \times 10^3$	$2.2 \times 10^3$	$5.2 \times 10^2$
San Andres Dolomite	$2.4 \times 10^6$	76,500	$1.9 \times 10^4$	$6.8 \times 10^3$	$8.5 \times 10^2$	$1.0 \times 10^2$	$1.3 \times 10^1$
San Andres Dolomite	$3.4 \times 10^6$	17,300	$9.4 \times 10^3$	$2.8 \times 10^3$	$2.5 \times 10^2$	$2.3 \times 10^1$	-

TABLE 6 - MEASURED ROCK EMBEDMENT STRENGTH OF VARIOUS DRY CARBONATE ROCKS

Formation	Rock Embedment Strength psi
Desert Creek B Limestone	42,000
San Andres Dolomite	50,000-175,000
Austin Chalk - Buda Limestone	20,000
Bloomberg Limestone	93,000
Caddo Limestone	38,000
Canyon Limestone	50,000-90,000
Capps Limestone	50,000-85,000
Cisco Limestone	40,000
Edwards Limestone	53,000
Indiana Limestone	45,000
Novi Limestone	106,000
Penn Limestone	48,000
Wolfcamp Limestone	63,000
Clearfork Dolomite	49,000-200,000
Greyburg Dolomite	75,000-145,000
Rodessa Hill Laminate	170,000
San Angelo Dolomite	100,000-160,000



A - Reaction rate limit is the upper bound on the acid penetration.



B - Fluid loss limit is the lower bound on the acid penetration.

Fig. 1 - Limiting aspects of conventional acid fracturing treatments.

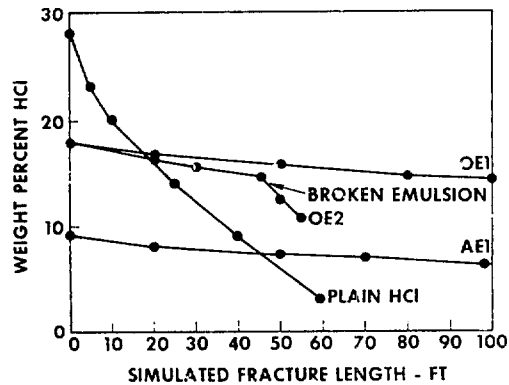


Fig. 4 - Experimentally measured acid concentration profiles along a fracture for HCl and emulsified acids.

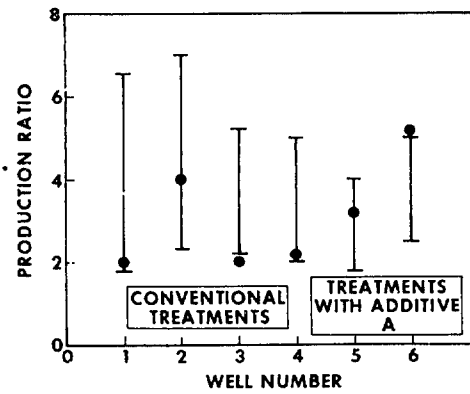


Fig. 2 - Comparison of conventional acid fracturing treatments to treatments using Additive A.

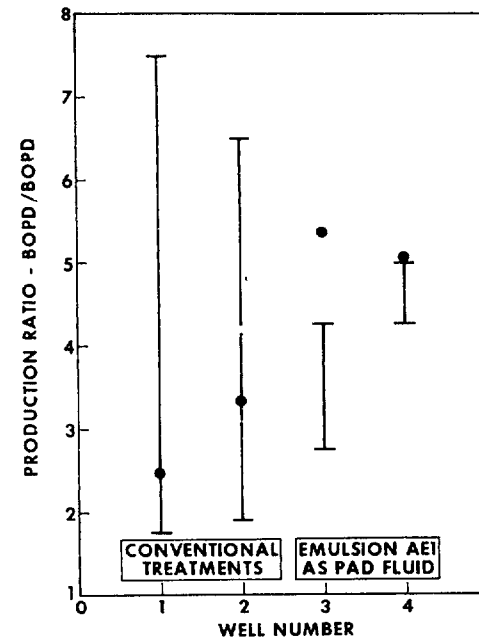


Fig. 3 - Comparison of conventional treatment results with acid external emulsion results.

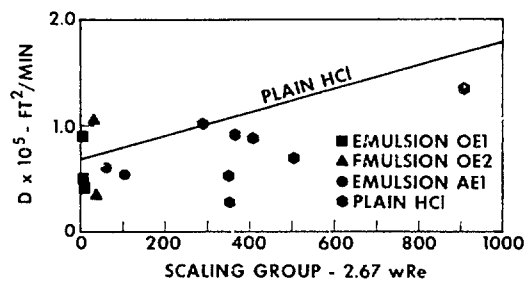


Fig. 5 - Effective mixing coefficient for various acid systems.

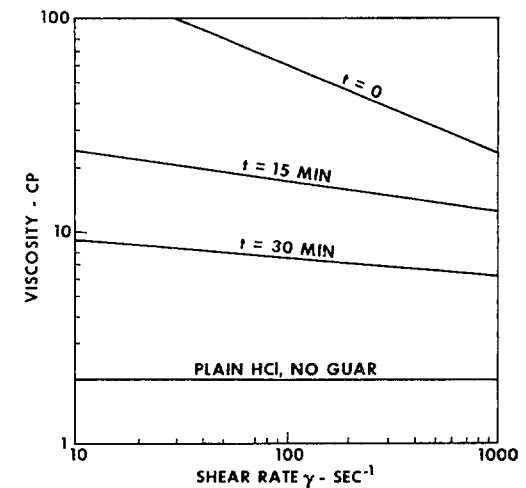


Fig. 6 - Viscosity of 15 percent HCl containing 50 lb guar/1,000 gal acid at 100°F.

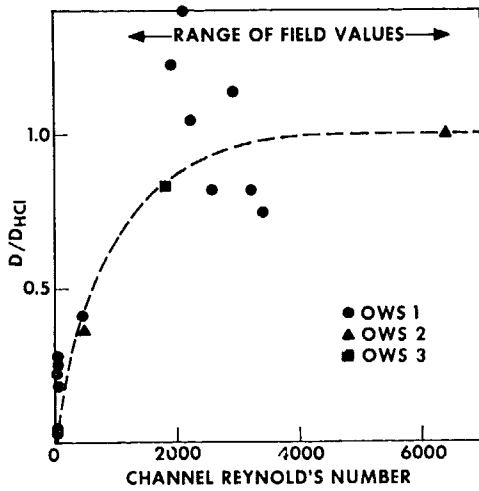


Fig. 7 - Mixing coefficients for oil wetting surfactants.

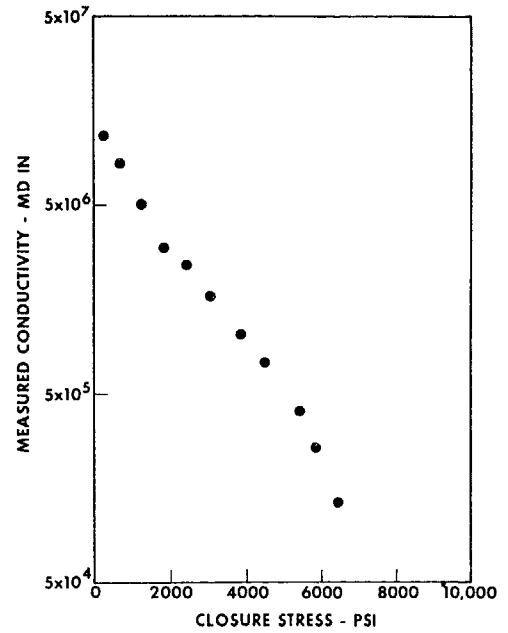


Fig. 8 - Typical conductivity vs closure stress for field core plug.

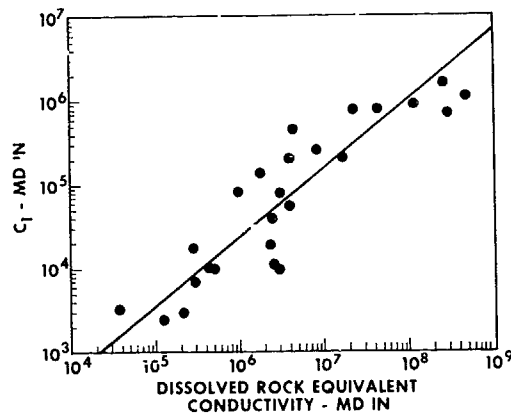


Fig. 9 - Correlation for  $C_1$  parameter of Eq. 1.

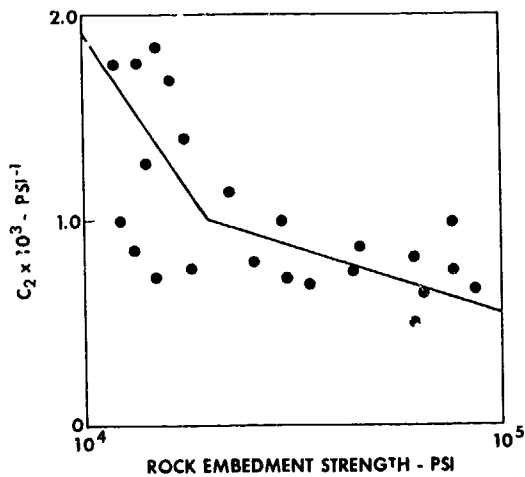


Fig. 10 - Correlation for  $C_2$  parameter in Eq. 1.

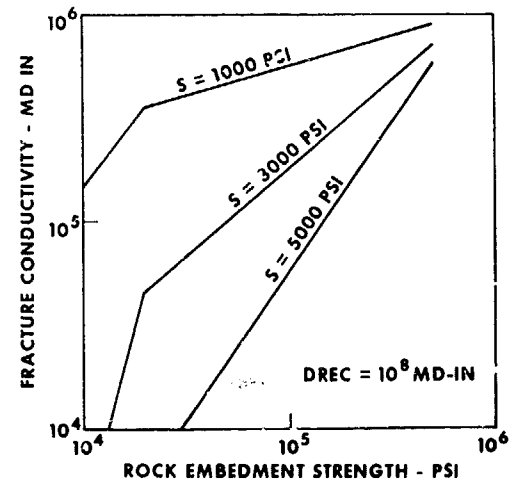


Fig. 11 - Fracture conductivity vs RES and closure stress.